


# Supplementary material for "Ultrafast relaxation of symmetry-breaking photo-induced atomic forces"

Shane M. O'Mahony,[1,2] Felipe Murphy-Armando,[2] Éamonn D. Murray,[3] José D. Querales-Flores,[2] Ivana Savić,[2] and Stephen Fahy[1,2]

[1] *Department of Physics, University College Cork, Cork T12K8AF, Ireland*
[2] *Tyndall National Institute, Cork T12R5CP, Ireland*
[3] *Department of Physics and Department of Materials, Imperial College London, London SW7 2AZ, United Kingdom*

(Dated: July 1, 2019)

This document serves as a supplement to the article "Ultrafast relaxation of symmetry-breaking photo-induced atomic forces". It contains details of the numerical convergence of the $E_g$ force lifetimes and the Wannier interpolation of the electronic bands. It also contains a detailed explanation of the modifications made to the experimental analysis in Ref. [1] and a derivation of the equation used for computing atomic forces in terms of the diagonal part of the electron-phonon matrix.

## I. WANNIER INTERPOLATION OF ELECTRON-PHONON MATRIX ELEMENTS

The electronic bandstructure, phonon dispersion and electron-phonon coupling matrix elements were calculated on a uniform $6\times6\times6$ Brillouin zone grid within the framework of density functional perturbation theory. We used a 25 hartree plane wave energy cutoff and the local density approximation to exchange and correlation. Norm-conserving pseudopotentials including spin orbit coupling were used for all 3 materials. These quantities were then interpolated to finer grids using maximally localised Wannier functions (MLWF) as implemented in the EPW code [2]. The interpolation of the electronic bandstructure of Bi, Sb and As are shown in Figs. 1, 2 and 3 respectively. These were performed using 14 Wannier orbitals for Bi and 16 Wannier orbitals for Sb and As. Since we consider photoexcited pump pulse photons between 0.5 eV and 3.0 eV, we are interested in states within $\sim 2$ eV of the Fermi level, which are well represented by this Wannier interpolation for all three materials.

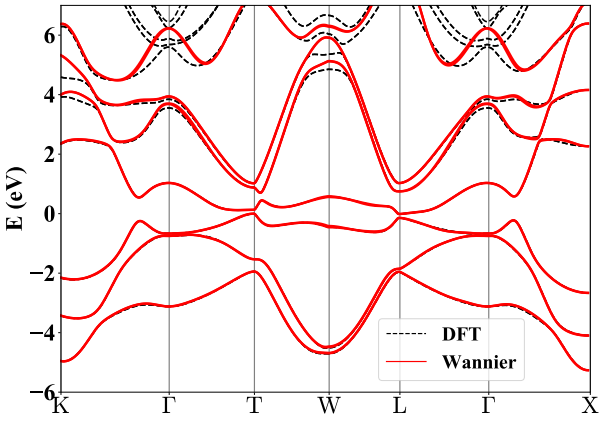


FIG. 1. Comparison of Bi DFT bands with those obtained by Wannier interpolation. 14 Wannier orbitals were used to interpolate the bandstructure from a coarse $6\times6\times6$ grid.

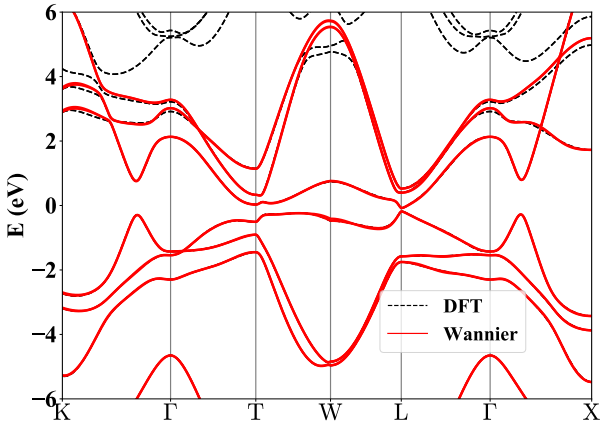


FIG. 2. Comparison of Sb DFT bands with those obtained by Wannier interpolation. 16 Wannier orbitals were used to interpolate the bandstructure from a coarse $6\times6\times6$ grid.

The electron-phonon matrix elements are interpolated from a coarse $6\times6\times6$ grid to finer grids.

## II. CONVERGENCE OF $E_g$ FORCE LIFETIMES

The $E_g$ force lifetime has two convergence parameters, the number of $k$(and $q$) points in the uniform Brillouin zone grid ($N_k$) and the Gaussian smearing, $\sigma$, used to compute $\mathrm{Im}\{\Sigma_{n\mathbf{k}}\}$ (see Eq. 4 of main text.). As shown in Fig. 4, the low-temperature (0.1 K) $E_g$ force lifetime at the experimental pump-pulse energy (1.5 eV) is insensitive to $\sigma$ and is converged at a Brillouin zone grid of $N_k = 12\times12\times12$. At a grid density of $N_k = 14\times14\times14$, the $E_g$ force lifetime converges in all 3 materials and at all temperatures considered, so we perform our calculations on that grid.

At excitation energies where the electronic density of states is very low, the convergence with respect to grid sampling becomes more demanding. However, for the

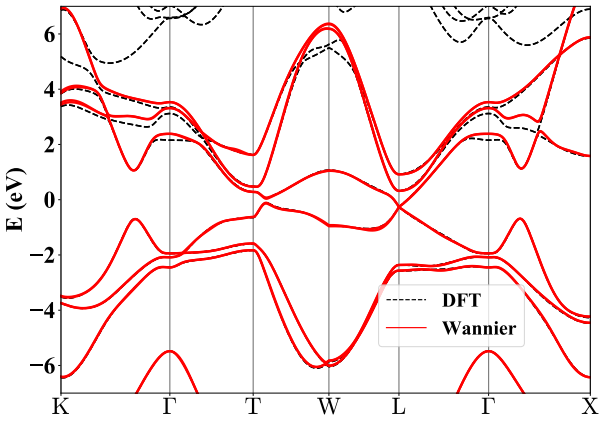


FIG. 3. Comparison of As DFT bands with those obtained by Wannier interpolation. 16 Wannier orbitals were used to interpolate the bandstructure from a coarse $6 \times 6 \times 6$ grid.

energy range shown in Fig. 3 of the main text, going from a $14 \times 14 \times 14$ grid to a $16 \times 16 \times 16$ grid makes at most a difference of $\sim 20\%$.

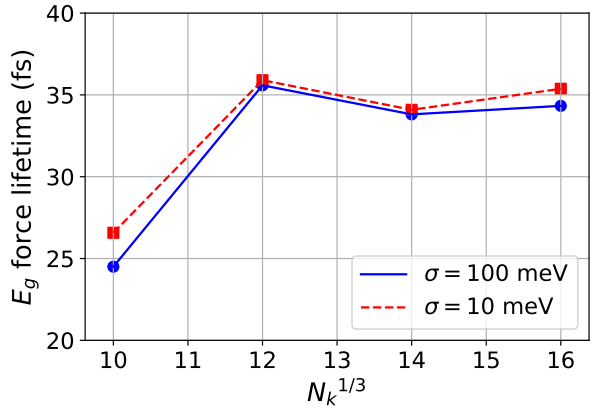


FIG. 4. Convergence of low-temperature (0.1 K) $E_g$ force lifetime in Bi with respect to $N_k$ and $\sigma$ assuming an absorbed photon energy of 1.5 eV.

## III. ANTIMONY $E_g$ FORCE DECAY RATE WITH ADDITIONAL TEMPERATURE-INDEPENDENT SCATTERING

The calculated and experimental values of the Sb $E_g$ force decay rate differ approximately by a temperature-independent scattering rate of $\Gamma' \sim 12.5$ ps$^{-1}$. Figure. 5 shows the calculated decay rate of the $E_g$ force on Sb, $\Gamma_{E_g}$, the experimental $E_g$ force decay rate and $\Gamma_{E_g} + \Gamma'$. It shows that the discrepancy between the calculated and measured $E_g$ force decay rate in Sb is consistent with a temperature-independent correction due to static imperfections, such as impurities or grain boundaries.

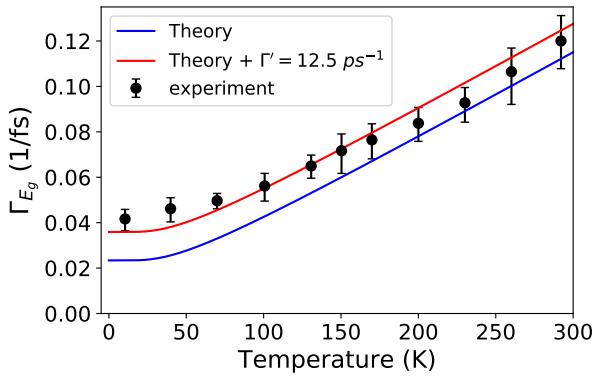


FIG. 5. Decay rate of $E_g$ force in Sb, including (red line) and excluding(blue line) a correction due to a temperature-independent scattering rate of $\Gamma' \sim 12.5$ ps$^{-1}$.

## IV. ANALYSIS OF EXPERIMENT INCLUDING PARTIAL DECAY OF $A_{1g}$ FORCE.

The relaxation time of the $E_g$ mode driving force in bismuth and antimony is experimentally determined by comparing the amplitudes of the $E_g$ and $A_{1g}$ modes obtained from a time-resolved optical pump-optical probe experiment and the corresponding cross sections obtained from cw Raman scattering [1]. The $A_{1g}$ mode driving force is assumed to remain constant for the duration of the pump pulse ($\sim 70$ fs).

However, our calculations show a partial decay of the $A_{1g}$ force from its initial value to a non-zero constant value on timescales much shorter than the pump-pulse duration. In order to estimate the impact of this on the experimentally derived $E_g$ force lifetime, we need to understand the amount by which this partial decay modifies the initial amplitude of the $A_{1g}$ mode.

At times much greater than the pump pulse duration ($t \gg \tau_p$) and assuming that the pump pulse duration is much less than the phonon period ($\Omega\tau_p \ll 1$), we can describe the $A_{1g}$ mode by a harmonic oscillator subject to 2 driving forces, a step function which decays at a rate $\Gamma$, and one which does not decay. This gives the following equation of motion :

$$\ddot{Q} + \Omega^2 Q = \frac{F_0}{\mu}[s + (1-s)e^{-\Gamma t}], \tag{1}$$

where $s \in [0, 1]$, $F_0$ is the initial driving force and $\mu$ is the effective mass. Making the substitution $Q \to \mu Q/F_0$, we arrive at the simpler equation:

$$\ddot{Q} + \Omega^2 Q = s + (1-s)e^{-\Gamma t}, \tag{2}$$

which has a general solution of the form:

$$Q(t) = A\cos(\Omega t + \phi) + \frac{s}{\Omega^2} + \frac{1-s}{\Gamma^2 + \Omega^2}e^{-\Gamma t}. \tag{3}$$

The initial conditions are that $Q(0) = 0$ and that $\dot{Q}(0) =$

0, which give us the following:

$$-A\cos(\phi) = \frac{s}{\Omega^2} + \frac{1-s}{\Gamma^2+\Omega^2} \tag{4}$$

$$-A\sin(\phi) = \frac{1-s}{\Gamma^2+\Omega^2}\left(\frac{\Gamma}{\Omega}\right). \tag{5}$$

Taking the ratio of these we obtain the phase:

$$\tan\phi = \frac{\Omega\Gamma(1-s)}{s\Gamma^2+\Omega^2}. \tag{6}$$

There are two important limits of this expression: when $s = 0$, we get $\tan\phi = \Gamma/\Omega$, which is the phase of the $E_g$ mode as shown in Ref. [1]; when $s = 1$, we get $\phi = 0$, which is the phase of the $A_{1g}$ mode given by DECP theory.

Summing the squares of Eq. (4) and Eq. (5), we find that the amplitude, $A = \Lambda/\Omega^2$, where $\Lambda$ is defined by:

$$\Lambda^2 \equiv \left[\frac{s^2}{\frac{\Omega^2}{\Gamma^2}+1} + \frac{1}{\frac{\Gamma^2}{\Omega^2}+1}\right] \tag{7}$$

This gives us the following equation of motion for the $A_{1g}$ mode:

$$Q(t) = \frac{1-s}{\Gamma^2+\Omega^2}e^{-\Gamma t} + \frac{\Lambda}{\Omega^2}\left[\frac{s}{\Lambda} - \cos(\Omega t+\phi)\right] \tag{8}$$

If we compare this with the equation of motion for the $A_{1g}$ mode driven by a **time-independent** force:

$$Q(t) = \frac{1}{\Omega^2}\left[1-\cos(\Omega t+\phi)\right], \tag{9}$$

we see that the effect of the force decaying from $F_0 \to sF_0$ is to reduce the amplitude of the $A_{1g}$ mode by the factor $\Lambda$.

## V. EFFECT ON DERIVED EXPERIMENTAL $E_g$ FORCE LIFETIME

Li et. al. gives the following expression for the $E_g$ force relaxation rate [1]:

$$\Gamma_{E_g} = \Omega_{E_g}\sqrt{\frac{{g_{PP}}^4}{{g_{RS}}^4} - 1}, \tag{10}$$

where ${g_{PP}}^4 = (A_{A_{1g}}\tilde{A}_{A_{1g}}/A_{E_g}\tilde{A}_{E_g})^2$ is the "effective electron-phonon coupling" from the optical pump-optical probe experiment and ${g_{RS}}^4 = (A_{A_{1g}}/A_{E_g})^4$ is the corresponding coupling deduced from cw Raman scattering cross sections which are insensitive to electronic decay of the mode driving forces. The amplitudes are assumed to be of the form [1]:

$$A_{E_g} = \frac{F^0_{E_g}}{\mu{\Omega_{E_g}}^2} \tag{11}$$

$$\tilde{A}_{E_g} = \frac{F^0_{E_g}}{\mu{\Omega_{E_g}}^2\sqrt{1+\frac{{\Gamma_{E_g}}^2}{{\Omega_{E_g}}^2}}} \tag{12}$$

$$A_{A_{1g}} = \frac{F^0_{A_{1g}}}{\mu{\Omega_{A_{1g}}}^2}. \tag{13}$$

The amplitude $\tilde{A}_{A_{1g}}$ is assumed to be approximately equal to $A_{A_{1g}}$, which amounts to assuming that the $A_{1g}$ driving force remains constant over the duration of the pump pulse ( $\sim$ 70 fs). Since our calculations show a partial decay of the $A_{1g}$ driving force in Bi and Sb, we make the following modification:

$$\tilde{A}_{A_{1g}} = \frac{F^0_{A_{1g}}\Lambda}{\mu{\Omega_{A_{1g}}}^2}, \tag{14}$$

which implies a change to the derived values of the $E_g$ force lifetime by a factor of:

$$\tau_{E_g} = \frac{\sqrt{\frac{{g_{PP}}^4}{{g_{RS}}^4} - 1}}{\sqrt{\Lambda^2\frac{{g_{PP}}^4}{{g_{RS}}^4} - 1}}. \tag{15}$$

Fig. 6 shows the resulting modifications to the experimentally derived $E_g$ force lifetimes for Bi and Sb:

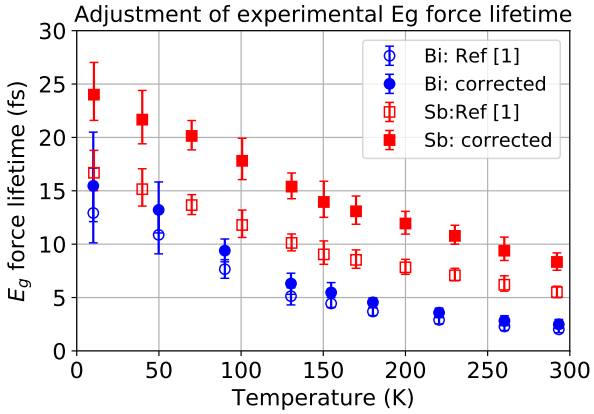


FIG. 6. Corrections to the experimentally derived $E_g$ force lifetimes reported in Ref [1]. The open points are the experimental values reported in Ref [1], the solid points are the experimental values after taking into account the calculated partial decay of the $A_{1g}$ driving force.

## VI. HAMILTONIAN FOR ELECTRON-PHONON SCATTERING

The Hamiltonian for the electron-phonon interaction is:

$$\boxed{H_{\text{eph}} = \left(\frac{\hbar}{2N}\right)^{\frac{1}{2}} \sum_{\mathbf{q},\lambda} \frac{a^{\dagger}_{-\mathbf{q}\lambda} + a_{\mathbf{q}\lambda}}{\sqrt{\omega_{\lambda}(\mathbf{q})}} \sum_{\mathbf{k},n,m} c^{\dagger}_{m\mathbf{k}+\mathbf{q}} c_{n\mathbf{k}}\, g^{\lambda\mathbf{q}}_{\mathbf{k}nm}}, \tag{16}$$

where $\omega_{\lambda}(\mathbf{q})$ is the frequency of the phonon with wavevector $\mathbf{q}$ and branch $\lambda$, $a_{\mathbf{q}\lambda}$ is the phonon annihilation operator, $c_{n\mathbf{k}}$ is the electron annihilation operator and $g^{\lambda\mathbf{q}}_{\mathbf{k}nm}$ is the electron-phonon matrix element defined as:

$$g^{\lambda\mathbf{q}}_{\mathbf{k}nm} = \sum_{\alpha} \frac{\mathbf{e}^{\lambda}_{\alpha}(\mathbf{q})}{\sqrt{M_{\alpha}}} \cdot \langle m\mathbf{k}+\mathbf{q}|\nabla_{\boldsymbol{\tau}_{\alpha}} V|n\mathbf{k}\rangle \tag{17}$$

where $N$ is the number of primitive cells in the system, $M_{\alpha}$ is the mass of the atom indexed by $\alpha$, $\mathbf{e}^{\lambda}_{\alpha}(\mathbf{q})$ is the phonon eigenvector of mode and $\nabla_{\boldsymbol{\tau}_{\alpha}} V$ is the derivative of the potential with respect to atomic displacement $\tau_{\boldsymbol{\alpha}}$ within the primitive cell.

## VII. $E_g$ AND $A_{1g}$ FORCES FROM ELECTRON-PHONON MATRIX ELEMENTS

Koopman's theorem relates the DFT total energy, $E_{\text{DFT}}$ to the energy and occupation of orbital $|n\mathbf{k}\rangle$ [3]:

$$\frac{\partial E_{\text{DFT}}}{\partial f_{n\mathbf{k}}} = E_n(\mathbf{k}) = \langle n\mathbf{k}|\hat{H}|n\mathbf{k}\rangle\,. \tag{18}$$

To first order in $\Delta f_{n\mathbf{k}}$, the change in the DFT total energy per unit cell is as follows:

$$\begin{aligned}\Delta E_{\text{DFT/cell}} &\approx \frac{1}{N}\sum_{n,\mathbf{k}} \Delta f_{n\mathbf{k}} \langle n\mathbf{k}|\hat{H}|n\mathbf{k}\rangle \\ &= \frac{1}{N}\sum_{n,\mathbf{k}} \left(f_{n\mathbf{k}} - f^{(0)}_{n\mathbf{k}}\right) \langle n\mathbf{k}|\hat{H}|n\mathbf{k}\rangle \end{aligned} \tag{19}$$

where $f^{(0)}_{n\mathbf{k}}$ is the equilibrium electronic occupation of the state $|n\mathbf{k}\rangle$ at the instantaneous temperature of the lattice and N is the number of unit cells in the system. In practice, we can set $f^{(0)}_{n\mathbf{k}}$ equal to the equilibrium occupation of state $|n\mathbf{k}\rangle$ before photoexcitation because the lattice temperature doesn't change substantially over the timescales being considered in this work ($\sim 10$ fs). The force $\boldsymbol{F}_{\boldsymbol{\alpha}}$ on atom $\alpha$ is then:

$$\begin{aligned} F_{\alpha i} &= -\nabla_{\boldsymbol{\tau}_{\alpha}}[\Delta E_{\text{DFT}}/\text{cell}] \\ &= -\frac{1}{N}\sum_{n,\mathbf{k}} \nabla_{\boldsymbol{\tau}_{\alpha}} \left[\Delta f_{n\mathbf{k}} \langle n\mathbf{k}|\hat{H}|n\mathbf{k}\rangle\right] \\ &\approx -\frac{1}{N}\sum_{n,\mathbf{k}} \Delta f_{n\mathbf{k}} \nabla_{\boldsymbol{\tau}_{\alpha}} \left[\langle n\mathbf{k}|\hat{H}|n\mathbf{k}\rangle\right] \end{aligned}$$

If we assume that the single-particle states $|n\mathbf{k}\rangle$ are eigenstates of $\hat{H}$, then we can apply the Hellman-Feynman theorem [4]. This allows us to express the forces in terms of the diagonal electron-phonon matrix elements and the occupations of the electronic states:

$$\boxed{F_{\alpha i} = -\frac{1}{N}\sum_{n,\mathbf{k}} \Delta f_{n\mathbf{k}} \langle n\mathbf{k}|\nabla_{\boldsymbol{\tau}_{\alpha}} \hat{H}|n\mathbf{k}\rangle} \tag{20}$$

## VIII. COMPARING TEMPERATURE DEPENDENCE OF $\tau_{E_g}$ AND $\langle\tau\rangle$

In the main text we note that the temperature dependence of the $E_g$ force lifetime $\tau_{E_g}$ and that of the non-equilibrium average state lifetime $\langle\tau\rangle$ are very similar. Both $\langle\tau\rangle$ and $\tau_{E_g}$ were fitted with the function $f(T) = f(0)/[1 + 2n_B(T, \Omega_0)]$, where $n_B(T, \Omega_0)$ is the Bose-Einstein occupation number for a mode frequency $\Omega_0$ at temperature $T$. The frequency $\Omega_0$ is a fitting parameter that quantifies the temperature dependence. Here we compare the values of $\hbar\Omega_0$ obtained by fitting $\tau_{E_g}$ ($\hbar\Omega_0(\tau_{E_g})$) with those obtained by fitting $\langle\tau\rangle$ ($\hbar\Omega_0(\langle\tau\rangle)$).

TABLE I. Comparison of fitting parameter $\hbar\Omega_0(\tau_{E_g})$ with $\hbar\Omega_0(\langle\tau\rangle)$, showing that the temperature dependence of $\tau_{E_g}$ is similar to that of $\langle\tau\rangle$ in all three materials considered.

| Material | $\hbar\Omega_0(\tau_{E_g})$ (meV) | $\hbar\Omega_0(\langle\tau\rangle)$ (meV) |
|---|---|---|
| Bismuth | 6.8 | 6.7 |
| Antimony | 10.7 | 10.8 |
| Arsenic | 15.5 | 16.2 |


[1] J. J. Li, J. Chen, D. A. Reis, S. Fahy, and R. Merlin, Phys. Rev. Lett. **110**, 047401 (2013).

[2] S. Poncé, E. Margine, C. Verdi, and F. Giustino, Computer Physics Communications **209**, 116 (2016).

[3] R. M. Martin, *Electronic Structure: Basic Theory and Practical Methods* (Cambridge University Press, 2004).

[4] R. P. Feynman, Physical Review **56**, 340 (1939).